IDŐJÁRÁS

Quarterly Journal of the Hungarian Meteorological Service
Vol. 120, No. 2, April – June, 2016, pp. 163–181

A closure study on aerosol extinction in urban air in Hungary

Ágnes Molnár [1*], **Dénes Párkányi** [2], **Kornélia Imre** [1], **Vera Gácser** [3], and **Edit Czágler** [4]

[1]*MTA-PE Air Chemistry Research Group, Veszprém, P.O.Box 158, H-8201 Hungary*

[2]*Centre for Energy Research, Hungarian Academy of Sciences, Budapest 114, P.O. Box 49, H-1525 Hungary*

[3]*University of Pannonia, Veszprém, P.O.Box 158, H-8201 Hungary*

[4]*Hungarian Meteorological Service, Budapest P.O. Box 39, H-1186 Hungary*

[*]*Corresponding author E-mail: amolnar@almos.uni-pannon.hu*

(Manuscript received in final form November 13, 2015)

Abstract—In this study, we present our results from an investigation into the use of visibility data as a viable tool for the survey of long-term variations in air quality. We found that visibility data in general can be used to estimate atmospheric aerosol extinction coefficients, and that PM_{10} can be successfully estimated from aerosol chemical composition. Our results indicate that PM_{10} concentrations provide a good basis for the reconstruction of aerosol extinction coefficients. It was also shown that both derived (from visibility) and reconstructed aerosol extinction coefficients were in good accordance with each other, mainly in the case of dry aerosols. Ambient values can be determined if an adequate hygroscopic growth rate for aerosol extinction is considered. We also found that a rather precise estimation of extinction coefficient can be reached if a modified version of the widely used IMPROVE formula is applied.

Key-words: visibility, reconstruction of extinction coefficient, PM_{10}, aerosol composition

1. Introduction

Visibility (VIS) is a good, simple indicator of air quality. It is well known that VIS is inversely related to atmospheric extinction. Light extinction is controlled by the scattering and absorption of air molecules and aerosol particles and is proportional to the number concentration of molecules and particles. The number of air molecules is a function of temperature and pressure; however, its variation does not result in a significant change in VIS. Drastic decreases or increases in visibility can be attributed to variations in aerosol concentration and changes in the physical and chemical properties of the particles.

According to the Koschmieder theory (*Koschmieder*, 1924), visibility is determined by

$$VIS = \frac{\ln 0.02}{\sigma_{ext}} = \frac{3.912}{\sigma_{ext}}. \quad (1)$$

In the formula, the constant of 3.912 represents the 2% contrast threshold of daylight visual detection of objects against the sky horizon, and σ_{ext} is the total extinction of solar radiation at 550 nm wavelength.

The scattering and absorption efficiencies of particles are functions of aerosol chemical composition and particle size. Sulfates, nitrates, and organics generally contribute to scattering, while elemental and organic carbon compounds are mainly responsible for absorption (e.g., *Malm et al.,* 1994; *Tao et al.,* 2012). Particles participate most in light extinction when their size is in the optically active size range (0.1–1.0 μm). On the other hand, the water vapor content of air (specifically relative humidity) has a significant influence on ambient light extinction as a consequence of water soluble and hygroscopic compounds in the aerosol. According to previous studies, hygroscopic growth can cause the scattering coefficient of dry particles to be doubled or greater as a result of increases in relative humidity (e.g., *Horvath,* 1992; *Seinfeld* and *Pandis,* 1998). Consequently, variations in aerosol concentration (through their size and chemical composition) control changes in dry extinction/visibility; however, in ambient air, water content can also play a major role in light attenuation and visibility impairment (e.g., *Jung et al.,* 2009; *Cheng et al.*, 2011).

High concentrations of air pollutants are a prevalent cause of air quality impairment in both cities and remote areas. Visibility can vary within a wide range, from a few meters to a few hundred kilometers (*Horvath,* 1995; *Singh* and *Dey*, 2012), and can easily become a critically important parameter in the everyday functioning of cities, because low visibility can obstruct surface and aerial traffic, and thereby, unfavorably impact businesses, public safety, and even tourism.

Despite the significant influence of water vapor, visibility (extinction) data provide an efficient and inexpensive tool for the study of long-term variations in air quality and may be utilized as a proxy for the concentration of aerosols and trace gases (*Singh* and *Dey*, 2012). For several decades, an empirical formula for calculating the light extinction coefficient as a function of chemical species in the $PM_{2.5}$ particulate matter has been used by the Interagency Monitoring of Protected Visual Environments (IMPROVE) network (*Hand et al.,* 2011; *Malm et al*, 2013). The IMPROVE program is a cooperative measurement effort among the U.S. Environmental Protection Agency (EPA), federal land management agencies, and state agencies (*Hand et al.,* 2011). The IMPROVE network has collected air quality data since 1988. The main goals of this program are to monitor real-time visibility and aerosol conditions in 156 mandatory Class I areas throughout the United States to identify aerosol species and their emission sources that are responsible for anthropogenic visibility impairment and to study and document long-term trends in air quality and visibility.

The empirical formula used by the IMPROVE network is based on the relationship between light extinction and aerosol chemical composition. The light extinction coefficients of an external mixture of aerosols can be estimated by assuming a linear combination of mass concentrations (M_j) and the corresponding extinction efficiencies (α_j) of different aerosol species (*Hand et al.,* 2011):

$$\sigma_{ext} = \sum \alpha_j \cdot M_j. \tag{2}$$

To account for the hygroscopic effect, extinction efficiencies are multiplied by a humidification factor that is computed by assuming a size distribution and a composition-dependent hygroscopic growth factor. The IMPROVE formula (see later Eq. (7)) is used to reconstruct σ_{ext} (corresponding to 550 nm wavelength) based on measurements of aerosol composition (ammonium sulfate, ammonium nitrate, particulate organic matter, light absorbing carbon, soil, and coarse mass) and a Rayleigh scattering term (*Hand* and *Malm*, 2007). The units of aerosol extinction coefficient and Rayleigh scattering are Mm^{-1}, mass concentrations are given in $\mu g\ m^{-3}$, and mass extinction (scattering and absorption) efficiencies have units of $m^2\ g^{-1}$.

The empirical IMPROVE formula has been applied extensively for different environments, from regional background to urban areas. An important issue is whether this algorithm, which is designed for background air, can be applied in cities. *Cabada et al.* (2004) found that by applying this formula during the Pittsburgh Air Quality Study, the scattering coefficient could be reproduced based on bulk $PM_{2.5}$ composition with relative success. Furthermore, in a number of studies, the extinction coefficient or visibility of megacities in China was reconstructed based on this formula. *Cao et al.* (2012) found that in

Xi'an, China, the model underestimated the measured extinction coefficient and that ammonium sulfate was the largest contributor. *Cheng et al.* (2011) in Jinan, *Pan et al.,* (2009) at a rural site near Beijing and *Tao et al.* (2012) in the Guangzhou urban area all concluded that the IMPROVE formula can provide realistic estimates of the real atmospheric extinction in cases where the relative humidity (RH) was less than 70% (*Tao et al.,* 2012). Under high RH, due to the hygroscopicity of the particles, the absorbed water plays a much greater role in limiting visibility. The study by *Singh* and *Day* (2012), conducted in the megacity of Delhi, India, resulted in similar conclusions. They found that below 80% RH, aerosols contribute ~90% to the observed visibility degradation, but that above 80% RH, the aerosol relative contribution decreases rapidly due to the strong impact of hygroscopicity. Visibility is most sensitive to water-soluble particles and soot in all seasons.

In this work, we studied and discussed the following issues:

a. How the extinction coefficient derived from visibility data can be estimated using the PM_{10} mass and chemical composition;

b. How PM_{10} can be reconstructed from the chemical composition of PM_{10};

c. How PM_{10} can be modelled from visibility observations. This information can result in a retrospective estimation of PM_{10} for periods when PM_{10} data are not available;

d. How the derived extinction coefficient (from VIS) corresponds to the reconstructed data;

e. Similar to other studies, we applied the IMPROVE formula in Budapest. We aimed to clarify how it can be applied in a Central European city and how the parameters in the formula should be changed to better reproduce the measured extinction coefficient;

f. How the hygroscopic effect should be considered to obtain a viable ambient extinction coefficient.

2. Experimental

2.1. Sampling

In this study, data from two sampling campaigns representing winter (February 2 – March 2, 2009) and summer (July 20 – August 20, 2009), aerosols are presented. In both cases, the sampling was conducted at the Marczell György Observatory of the Hungarian Meteorological Service. This site is located in the south-eastern part of Budapest, Hungary. Here, at a standard synoptic weather station, meteorological parameters, including visibility, temperature, and dew point temperature, are measured on an hourly basis. Visibility is also determined

by visual observation. In the observatory, there is also an urban background air pollution monitoring site operated by the Hungarian Air Quality Network (www.levegominoseg.hu), which provides PM_{10} mass concentration. PM_{10} is monitored using the β-gauge method (*Chueinta* and *Hopke*, 2001).

In addition to these routine measurements, aerosol samples were collected daily to determine their chemical composition. A two-stage multi-jet impactor was applied at a sampling rate of 20 $Lmin^{-1}$. The PM_1 fraction was collected on quartz filters, and $PM_{1\text{-}10}$ was sampled on Al-foils. From these samples, the inorganic ion (sulfate, nitrate, chloride, ammonium, sodium, potassium, and magnesium) and total carbon contents were measured. Inorganic ion content was determined by ion chromatography (Dionex, 2120) with a detection limit below 10 ppb. The total carbon concentrations of the aerosol samples were measured using an Astro Model 2100 TOC analyzer. This method is based on NDIR absorption. The detection limit of these measurements was 2 μg C.

In the winter campaign, the scattering coefficient of aerosol at 550 nm was also monitored using an M903 integrating nephelometer calibrated with carbon dioxide. These data were used to reconstruct the scattering coefficient (see in Section 3.3). Unfortunately, in the summer campaign, this measurement was not available due to instrument failure. In both campaigns, the daily average absorption coefficients of the aerosol samples were determined indirectly. We supposed that the majority of absorbing components (soot) can be found in the PM_1 aerosol. Using the PM_1 quartz filters, the absorbance of the samples was determined (Eq. (3)). The light transmittance of blank and exposed filters was measured by PSAP (particle soot absorption photometer) at 550 nm. Their ratio gave transmittance (T), and absorbance (A) was derived by

$$A = \log\left(\frac{1}{T}\right). \tag{3}$$

Considering the air volume (V) and surface (S) of the filter, the average absorption coefficient was estimated:

$$\sigma_a = \frac{A \times S}{V}. \tag{4}$$

This method was checked with parallel measurements. During the summer campaign, a PSAP was operated to directly monitor the absorption coefficient. Using the same PSAP, the absorption coefficient was measured both directly and indirectly. From the direct measurements, the daily average absorption coefficients are calculated and compared to the absorption coefficients resulted from the indirect method. The results of this comparison are shown in *Fig. 1*. One can conclude that the absorption coefficients determined in both ways are

linearly related, as the average difference between them was 2.16 ± 2.39 Mm^{-1}. This means that the absorption coefficient was slightly overestimated (less than 10%) when it was calculated using the transmittance of the aerosol filter.

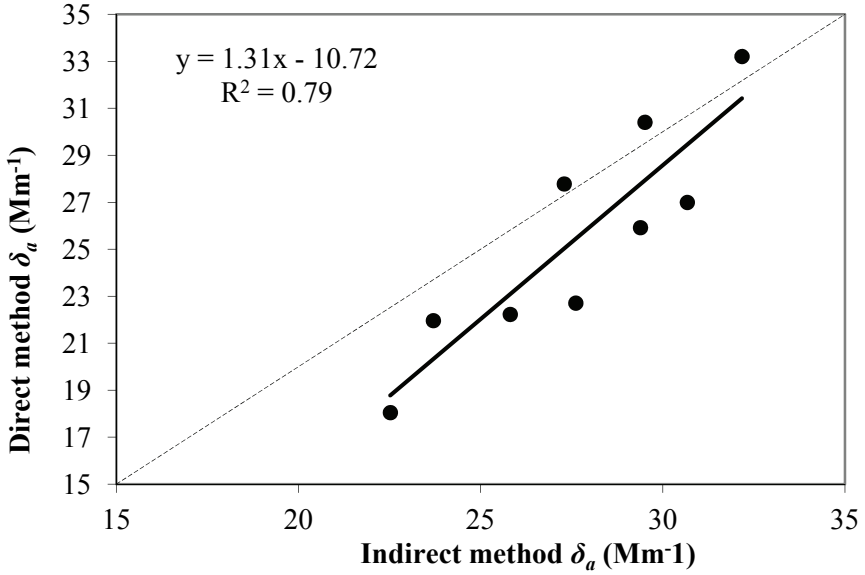

Fig. 1. Comparison of directly and indirectly measured absorption coefficients.

Finally, the organic and elemental (light absorbing) carbon contents of the samples were differentiated. We assumed that the total carbon content of the aerosol would be composed of organic and elemental fractions and that the inorganic carbon would be negligible (see in detail in Section 3.1). The elemental fraction was estimated from the absorption coefficient, considering a mass absorption coefficient of 10 m^{2}g^{-1}. Additionally, organic carbon was calculated as the difference between the total carbon (TC) and elemental carbon concentrations.

2.2. Extinction coefficient and the effect of hygroscopicity

Visibility (VIS) is generally determined by the light extinction of aerosol particles and air molecules. The extinction coefficient (σ_{ext}) can be estimated by means of Koschmieder theory (see Eq. (1)) which refers to 550 nm wavelength.

As previously mentioned, due to the hygroscopicity of the particles, relative humidity also plays an important role in determining visibility. The hygroscopic effect was excluded from the data sets by using the γ-approach as described by, e.g., *Zhou et al*. (2001):

$$\sigma_e = 10^c \times \left(1 - \frac{RH(\%)}{100}\right)^{-\gamma}, \tag{5}$$

$$f(RH) = \sigma_{RH}/\sigma_{40\%}. \tag{6}$$

We found that hygroscopic growth of the extinction coefficient (Eq. (6)) derived from VIS data was substantially different in winter and summer, as shown in *Table 1*. In winter, the aerosol was found to be much more hygroscopic than in summer, and the increase in the particle growth rate with rising RH was considerably greater than that in summer (e.g., at 80% RH, the growth rate was twice as much in winter than summer). As a result, considering the same PM_{10} concentrations, this difference yields a doubled extinction coefficient in winter compared with the summer values.

Table 1. Hygroscopic growth rate of extinction coefficients as a function of relative humidity

Relative humidity (%)	Winter	Summer	Winter/Summer
40	1.0	1.0	1.0
50	1.2	1.1	1.1
60	1.6	1.2	1.2
70	2.2	1.4	1.5
80	3.4	1.7	2.0
90	7.3	2.3	3.1

3. Results and discussion

3.1. Chemical composition and reconstruction of PM_{10}

The PM_{10} mass concentration was more variable during the winter campaign. In winter and summer, the average PM_{10} concentrations were 32 μgm^{-3} and 23 μgm^{-3}, respectively, with maximum concentrations of 107 μgm^{-3} and 54 μgm^{-3}. These average concentrations do not differ significantly from those obtained in three Austrian cities (*Gomišček et al.,* 2004), and Bologna, Italy (*Matta et al.,* 2003). In Vienna, Linz, Graz, and Bologna, the winter and summer PM_{10} concentrations varied in the ranges of 27–39 μgm^{-3} and 17–26 μgm^{-3}, respectively (*Gomišček et al.,* 2004; *Matta et al.,* 2003). In Lens, France (*Waked et al.,* 2014), the overall PM_{10} concentrations were lower, and in winter and summer, the values were 20 μgm^{-3} and 14 μgm^{-3}, respectively. Chemical analysis showed that in Budapest, carbonaceous compounds dominated the PM_{10} compositions, and the mass fractions of organic compounds in winter and summer were 35% and 27%, respectively. In Bologna and Lens, the mass fraction of organic carbon in PM_{10} was rather similar to that of Budapest (Bologna: winter 35% and summer 37% (*Matta et al.,* 2003); Lens: winter 34% and summer 27% (*Waked et al.,* 2014)). In contrast, in Budapest, elemental carbon represented 13% and 14% of PM_{10}, which was generally higher than the EC/BC data published for the other urban background sites around Europe. In

Barcelona, London North Kensington, Lugano (*Reche et al.,* 2011), Bologna (*Matta et al.,* 2003), and Lens (*Waked et al.,* 2014), the mass fractions of EC/BC in PM_{10} were in the range of 4%–10%.

In Budapest, the inorganic compounds were 16% (winter) and 18% (summer) of the total PM_{10} mass. These results are in accordance with earlier results obtained for PM_{10} in Budapest (*Maenhaut et al.,* 2005), but they are significantly lower than those found in other cities. It was found that in winter and summer in Bologna, inorganic species were 53% and 41% of PM_{10} (*Matta et al.,* 2003), while in Lens their contributions were 52% and 42% (*Waked et al.,* 2014).

During both campaigns in Budapest, all components analyzed from the filters were found dominantly in PM_1 as shown in *Table 2*. Among inorganic ions, nitrate was dominant in winter, whereas in summer, sulfate was found in highest concentrations, which is similar to results obtained in other cities. In Bologna, nitrate concentrations were almost 3 times higher than those of sulfate (*Matta et al.,* 2003), whereas in Lens, nitrate was twice as high as sulfate (*Waked et al.,* 2014). The lower nitrate concentrations in summer are the result of the temperature dependency of ammonium nitrate volatility, which was also indicated by lower nitrate fractions among the fine mode compared with the values obtained in winter. Yearly increases in sulfate concentrations during summer months are already known (e.g., *Hidy et al.,* 1978). Higher photochemical activities in summer result in higher rates of SO_2 conversion, which yield summertime maximums in sulfate concentrations. *Table 2* shows that the contributions of fine sulfate, ammonium, and total carbon to PM_{10} were significantly higher during summer than in winter. In contrast, the other components were less accumulated in PM_1 in summer than winter. Specifically, the fraction of fine nitrate concentration decreased from 80% (winter) to 70% (summer).

Table 2. PM_{10} aerosol composition and PM_1 mass fractions (%). The standard deviation is given in parentheses.

	Winter		**Summer**	
	Concentration (μgm^{-3})	**Fraction in PM_1 (%)**	**Concentration (μgm^{-3})**	**Fraction in PM_1 (%)**
chloride	2.4 (4.4)	85 (15)	1.1 (1.2)	77 (17)
nitrate	7.1 (3.6)	80 (12)	2.2 (0.9)	70 (8)
sulfate	4.2 (2.8)	80 (12)	6.2 (2.7)	93 (4)
sodium	2.0 (0.9)	95 (7)	1.4 (1.3)	65 (30)
ammonium	1.6 (1.6)	82 (17)	0.9 (0.5)	94 (13)
potassium	0.6 (0.3)	96 (5)	0.7 (0.5)	77 (18)
magnesium	0.1 (0.1)	85 (14)	0.2 (0.1)	71 (10)
calcium	1.3 (0.6)	81 (14)	1.7 (0.9)	69 (13)
total carbon	12.5 (6.6)	81 (4)	6.5 (1.2)	88 (7)

The total carbon concentration was twice as much in winter than in summer, and in both seasons more than 80% of the total carbon (TC) concentration was found in PM_1 (see *Table 1*). It is supposed that fine TC is composed primarily of organic and elemental carbon, and that the contribution of inorganic carbon (carbonate) can thus be neglected (e.g., *Karanasiou et al.,* 2011). Carbonate may be present in the coarse fraction; however, its presence has not been ubiquitously confirmed. According to a European survey (*Sillanpää et al.,* 2005), among six cities (Duisburg, Prague, Amsterdam, Helsinki, Barcelona, and Athens), carbonate was detected in the coarse mode in only the two Mediterranean cities. It should be mentioned that in Barcelona and Athens, the coarse fraction of the aerosol was greater than fine, whereas in Duisburg, Prague, and Amsterdam, similarly to Budapest, the fine mode dominated. Other results obtained for Chinese cities also showed the inorganic carbon (carbonate) content of the aerosol to be rather low (*Wang et al.,* 2010). Considering these results, we neglected the contribution of inorganic carbon in both the fine and coarse size ranges. Upon further evaluation, we supposed that the total carbon of PM_{10} was composed of organic and elemental (light absorbing) carbon and that this latter could be exclusively found in the fine fraction (PM_1).

The aerosol chemical composition was reconstructed on the basis of PM_{10}, and the inorganic and carbonaceous compounds were all considered. The chemical mass closure of the inorganic constituents was based on stoichiometry. In addition, based on the recommendations of *Stelson* and *Seinfeld* (1981), other alkaline (potassium) and alkaline earth metallic (calcium and magnesium) ions were included in the reconstruction of the PM_{10} mass. Excess nitrate was assumed to be organic nitrate (e.g., *Fry et al.,* 2014), and the organic and elemental carbon mass concentrations were estimated using conversion factors of 1.4 and 1, respectively. The average chemical composition of the reconstructed aerosol is shown in *Fig. 2*. It should be mentioned that in summer, the inorganic fraction of the aerosol was composed mainly of sulfate containing compounds. In contrast, during the winter season, nitrate compounds dominated the inorganic aerosol fraction, and sulfates (generally in the form of ammonium sulfate) gave a smaller contribution.

Finally, the reconstructed and the directly measured PM_{10} (by the β-gauge monitor described in Section 2.1) mass concentrations were compared. *Fig. 3* shows that these mass concentrations agreed relatively well in both sampling campaigns. In winter, PM_{10} is overestimated by 3.2 $\mu g m^{-3}$, whereas in summer, the directly measured PM_{10} is slightly lower than the reconstructed value.

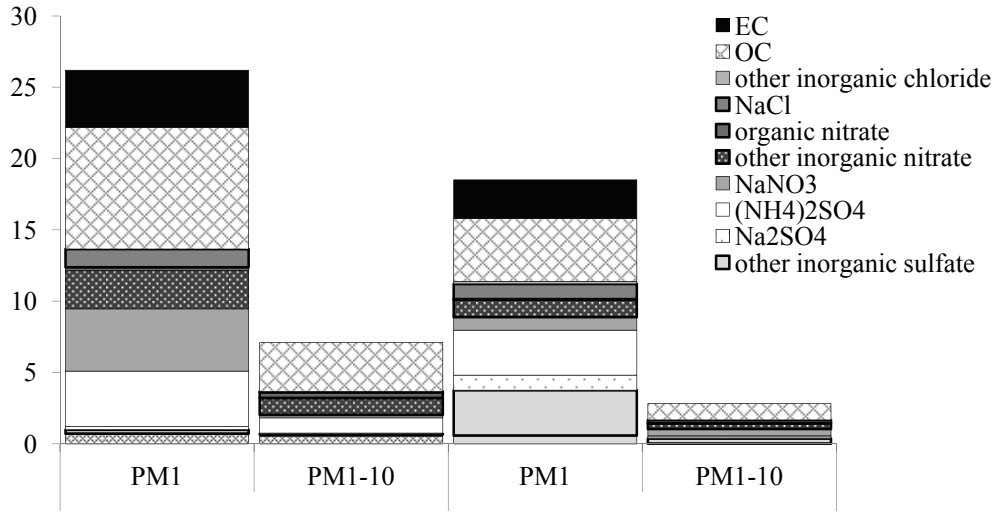

Fig. 2. Chemical mass closure of PM_1 and $PM_{1\text{-}10}$ in Budapest.

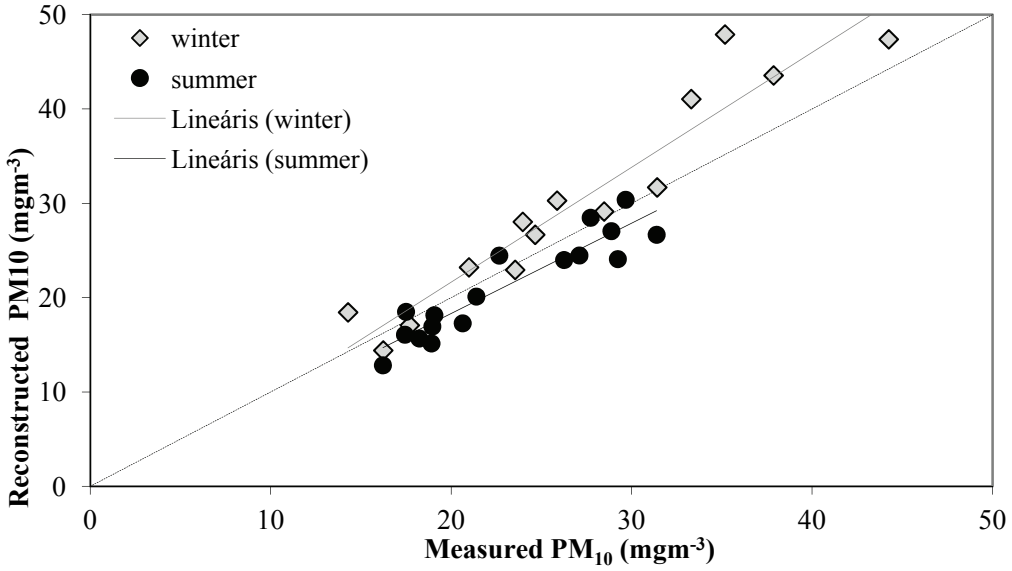

Fig. 3. Reconstructed vs. measured PM_{10} concentration.

3.2. Visibility and extinction coefficient (VIS, $\sigma_{e,VIS}$)

Temporal variations in PM_{10}, visibility, and RH are presented in *Figs. 4a* (winter) and *4b* (summer). The relationship among the parameters is clear. Low visibility coincides with high PM_{10} concentrations and/or high RH; conversely, high visibility occurs when PM_{10} and RH are low. As an example, in *Fig. 4a*, one can follow the development of a winter air pollution episode beginning on February 18 and finishing on February 25. Parallel to a general increase in PM_{10} (occasionally exceeding 100 μgm^{-3}), visibility decreased (average VIS = 7 km),

which was disrupted by a change in RH. In summer, aerosol aging processes also influence variations in visibility. *Bäumer et al.* (2008) demonstrated that when the prevailing air mass undergoes an aging process, and as a result, a significant decrease in VIS is observed, an increase in PM_{10} can be detected.

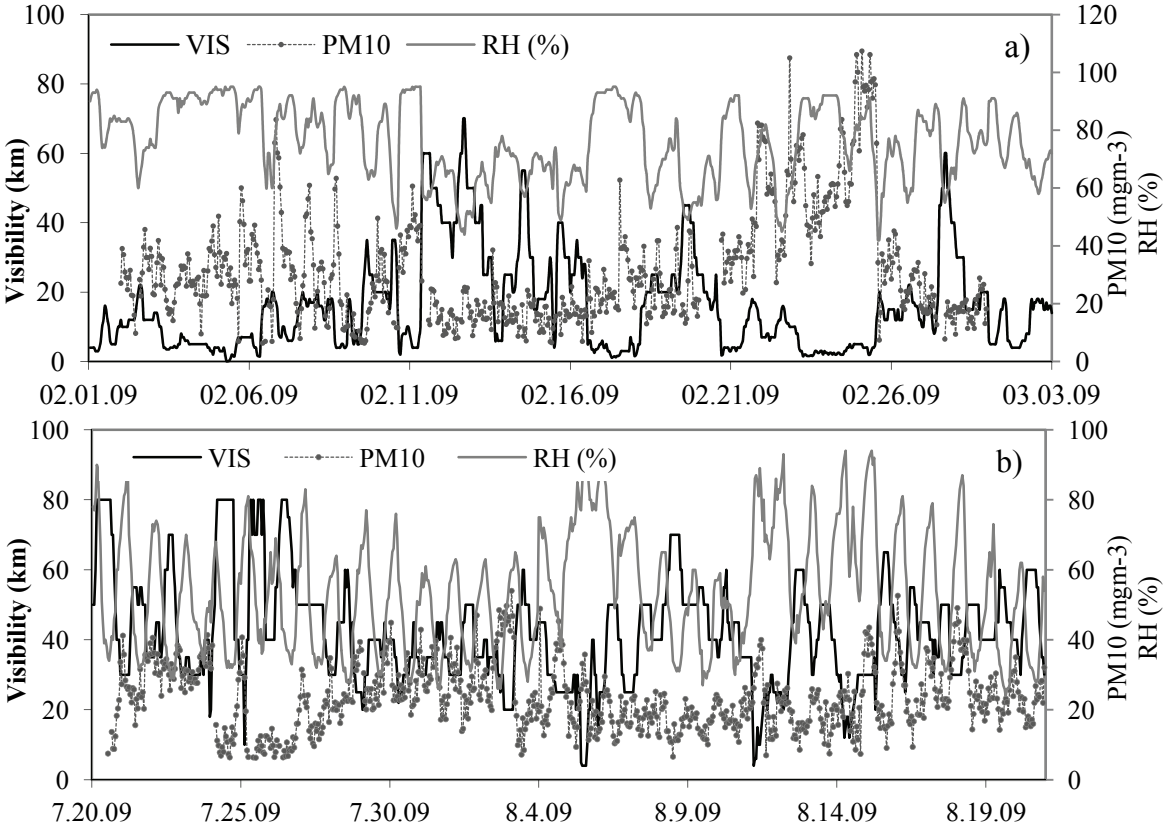

Fig. 4. Temporal variation in VIS, PM_{10} and RH during winter (a) and summer (b) campaigns.

In *Figs. 5a* and *5b*, temporal variations in the ambient and dry extinction coefficients are presented. The ambient extinction coefficients were derived from VIS (Eq. (1)), whereas the dry extinction data referring to 40% RH was obtained by means of the γ-approach (see Eqs. (5) and (6) in Section 2.2). In winter and summer, the average ambient extinction coefficients were 550 Mm^{-1} and 103 Mm^{-1}, and the dry average values were 126 Mm^{-1} and 87 Mm^{-1}, respectively. The difference between the ambient and dry extinction coefficients is attributed to the hygroscopic behavior of the aerosol. The effect of hygroscopicity on the aerosol extinction was particularly important in winter (see *Fig. 5a* and *Table 1*). The significant variation in hygroscopic growth rate is assumed to be the result of seasonal changes in PM_{10} chemical composition.

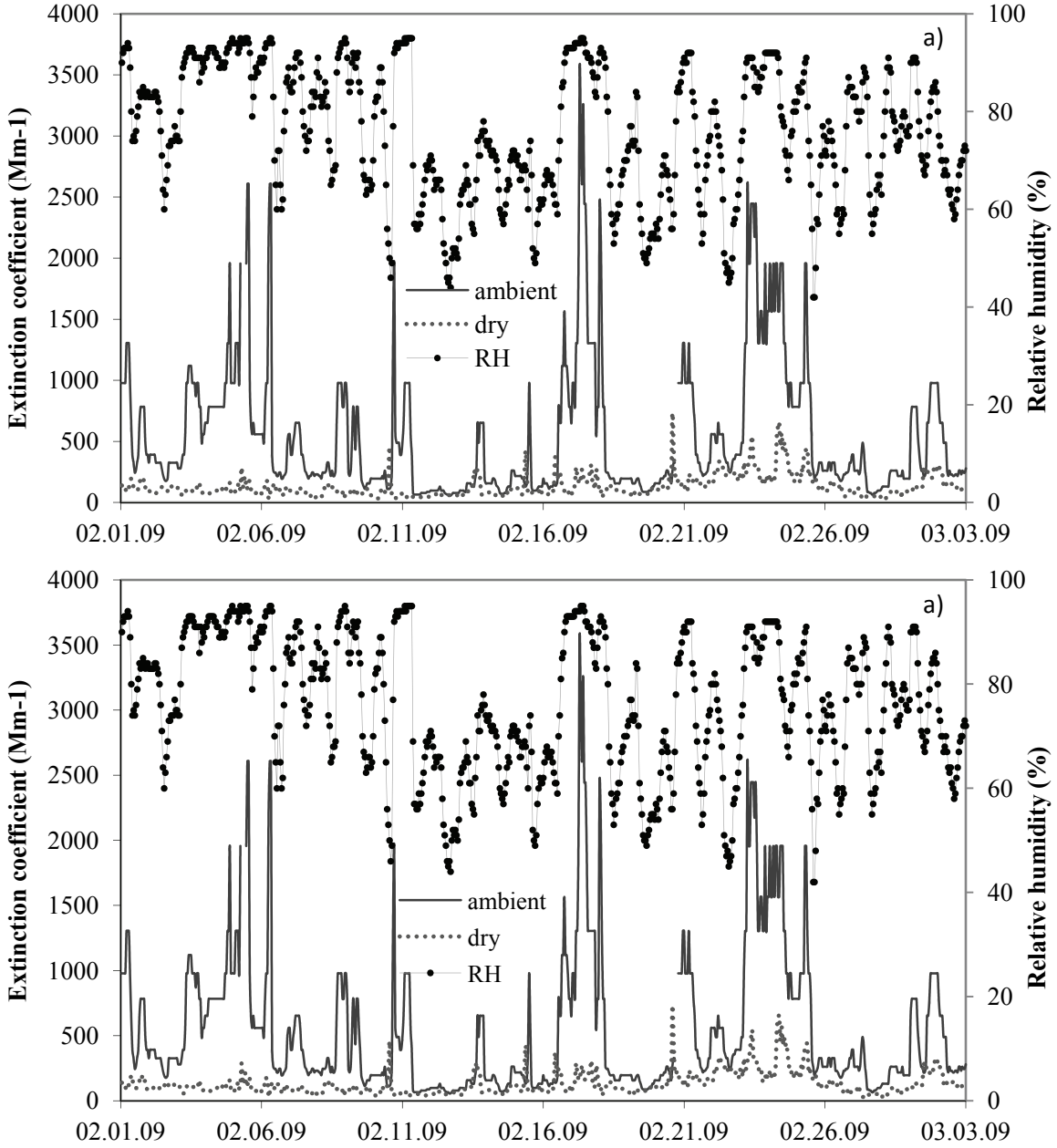

Fig. 5. Temporal variation in the ambient and dry extinction coefficients during winter (a) and summer (b) campaigns in 2009.

The relationship between PM_{10} and dry extinction coefficient is presented in *Fig. 6*. In both seasons, dry extinction coefficient varied similarly as a function of PM_{10}. Based on a linear regression analysis of the combined data sets, the dry mass extinction efficiency was 2.2 m^2g^{-1}, with a correlation coefficient of 0.52. This value is in accordance with the mass extinction efficiencies found in typical continental air. According to *Nemuc et al.* (2013), the mass extinction efficiencies of PM_{10} are typically in the range of 2.2 and 2.7 m^2g^{-1}, which was further confirmed by the value of 2.6 m^2g^{-1} that was obtained at the Hyytiälä Forestry Field Station in central Finland (*Virkkula et al.,* 2011).

Moreover, in urban air, the mass extinction coefficients of PM_{10} do not differ significantly from those obtained for background air. For reference, *Kim* (2015) and *Jung et al.* (2009) reported mass extinction efficiencies of 2.7 m^2g^{-1} and 2.5 m^2g^{-1} for Seoul, Korea, and Beijing, China, respectively.

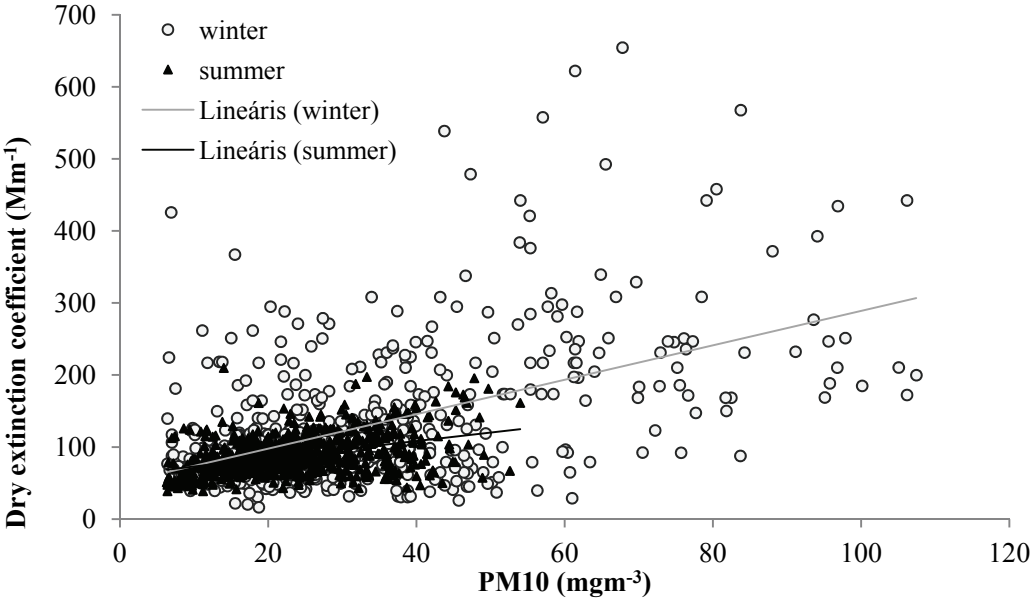

Fig. 6. PM_{10} vs. dry extinction coefficient during the winter and summer campaigns. The relationship between the parameters is statistically significant (at p=99.9%).

3.3. Reconstruction of extinction coefficient

The reconstruction of extinction coefficients is based on the well-known relationship between light extinction and aerosol composition. Sulfate, nitrate, and organic constituents have greater importance in scattering, whereas elemental carbon is more responsible for light absorption. Based on the concentration of different compounds and their mass extinction efficiencies, the extinction coefficient can be estimated (see Eq. (2)) (*Ouimette* and *Flagan*, 1982; *Mészáros*, 1999, *Seinfeld* and *Pandis*, 1998). This method has been well applied for a long time by the IMPROVE program (*DeBell et al.,* 2006) using the following equation:

$$\sigma_e \approx 3 \times f \times \left[(NH_4)_2SO_4\right] + 3 \times f \times \left[NaNO_3\right] + 4 \times \left[OC\right] + 10 \times \left[EC\right] + 1 \times \left[groundbased\right] + 0.6 \times \left[coarse\right] + 10 \times (Rayleigh). \quad (7)$$

To reconstruct the ambient extinction coefficient, the dry extinction coefficient was first estimated. In the estimation, we used aerosol chemical composition and optical data, which were independently monitored from visibility. In winter, aerosol scattering and absorption coefficients were measured along with visibility by integrating a nephelometer and PSAP (see

details in Section 2.1). The dry aerosol scattering coefficient was measured by the nephelometer and calculated using the gamma approach (Eq. (5)) that is used when estimating visibility. To estimate dry aerosol scattering, the main aerosol components including ammonium sulfate, ammonium, sodium, and other nitrates as well as organic compounds were taken into account. Multiple regression analysis was applied to determine mass scattering efficiencies. In addition to scattering, aerosol absorption was considered, and EC was calculated from the absorption coefficients of the aerosol daily samples (see details in Section 2.1.). Finally, Rayleigh scattering, which is a function of air temperature and pressure, was determined. We found that the reconstructed dry extinction coefficient can be calculated with the following equation:

$$\sigma_{dry} \approx 2.3 \times \left[(NH_4)_2SO_4\right] + 1.7 \times \left[NaNO_3 + KNO_3 + Ca(NO_3)_2 + Mg(NO_3)_2\right] + 1.5 \times \left[OC\right] + 10 \times \left[EC\right] + 12\left(Rayleigh\right). \quad (8)$$

When comparing the mass scattering/absorption efficiencies used in the IMPROVE network to our results, some similarities and differences were noticed. Our equation refers to PM_{10}, whereas in the IMPROVE network, $PM_{2.5}$ and coarse particles are considered separately. The mass scattering efficiencies of ammonium sulfate and nitrate salts were rather similar ($\approx 2\ m^2g^{-1}$) to those identified by the IMPROVE network ($3\ m^2g^{-1}$), although our obtained value was 30% smaller. In contrast to the inorganic species, the difference in mass scattering efficiencies for the organics is quite high (this study: $1.5\ m^2g^{-1}$; IMPROVE: $4\ m^2g^{-1}$). One possible explanation for the smaller values could be the difference between PM_{10} and $PM_{2.5}$, not differentiated in this study.

In addition, for the sake of simplicity, we modeled the dry extinction coefficient on the basis of only sulfate and nitrate ion as well as, organic and elemental carbon concentrations. In this case, the reconstruction equation was

$$\sigma_{dry,anions} = 4.3 \times \left[SO_4^{2-}\right] + 1.3 \times \left[NO_3^{-}\right] + 1.5 \times \left[OC\right] + 10 \times \left[EC\right] + 12\left(Rayleigh\right). \quad (9)$$

Comparing our models (Eqs. (8) and (9)) to the IMPROVE model (Eq. (7)), we concluded that all three models gave similar results for the reconstruction of the dry extinction coefficient. In *Table 3* the relationships between reconstructed and "observed" (calculated from visibility) extinction coefficients are shown. These relationships are characterized by linear regression equations and correlation coefficients. On the basis of these parameters, one can conclude that dry extinction data can be almost equally reconstructed by all three models. In other words the IMPROVE model – which is constructed for background aerosol – also provides sufficiently good estimation of dry extinction coefficient even in urban air, in Budapest. This is in agreement with other studies which

indicated similar conclusions in megacities of Beijing and Delhi: in relatively dry atmosphere, this model provided realistic estimation of the ambient extinction coefficient (*Tao et al.*, 2012; *Sing* and *Day*, 2012). It has to note, that our models (mainly Eq. (9)) require less input data than the IMPROVE model; and for this reason they can be more easily applied for the available data sets.

Table 3. Relationship between reconstructed (three models) and "observed" extinction coefficients

	Linear regression equation	**Correlation coefficient**
Dry aerosol		
Eq. (8)	y = 0.65x+10.4	0.577
Eq. (9)	y = 0.64x+20.5	0.619
IMPROVE	y = 0.76x+11.0	0.562
Ambient aerosol		
Eq. (8)	y = 0.96x-27.9	0.926
Eq. (9)	y = 0.97x-16.7	0.935
IMPROVE	y = 0.24x+53.7	0.779

Note: x and y are the extinction coefficient from VIS and the reconstructed (by models) extinction coefficients, respectively.

To reconstruct the ambient extinction coefficient, the hygroscopic growth of the extinction coefficient obtained from visibility data was calculated as:

$$\sigma_{ambient} = f \cdot \sigma_{dry}. \quad (10)$$

Then, the inorganic (sulfate and nitrate salts (Eq.8) or ions (Eq.9)) and organic (OC) parts in our models were multiplied by these growth factors (*f*). The adequacy of the models for the reconstruction of ambient extinction coefficients is shown in *Table 3*. In each season, the adequate hygroscopic growth rates were considered. We can conclude that both approaches are suitable for the reconstruction of the extinction coefficient; however, they slightly underestimate the ambient extinction coefficient when compared to visibility data.

Figs. 7a and *7b* show the agreement of ambient extinction in more detail. We can conclude that the temporal variation in the ambient extinction coefficient is well represented by both models, but the actual extent of σ is generally underestimated by the model equations.

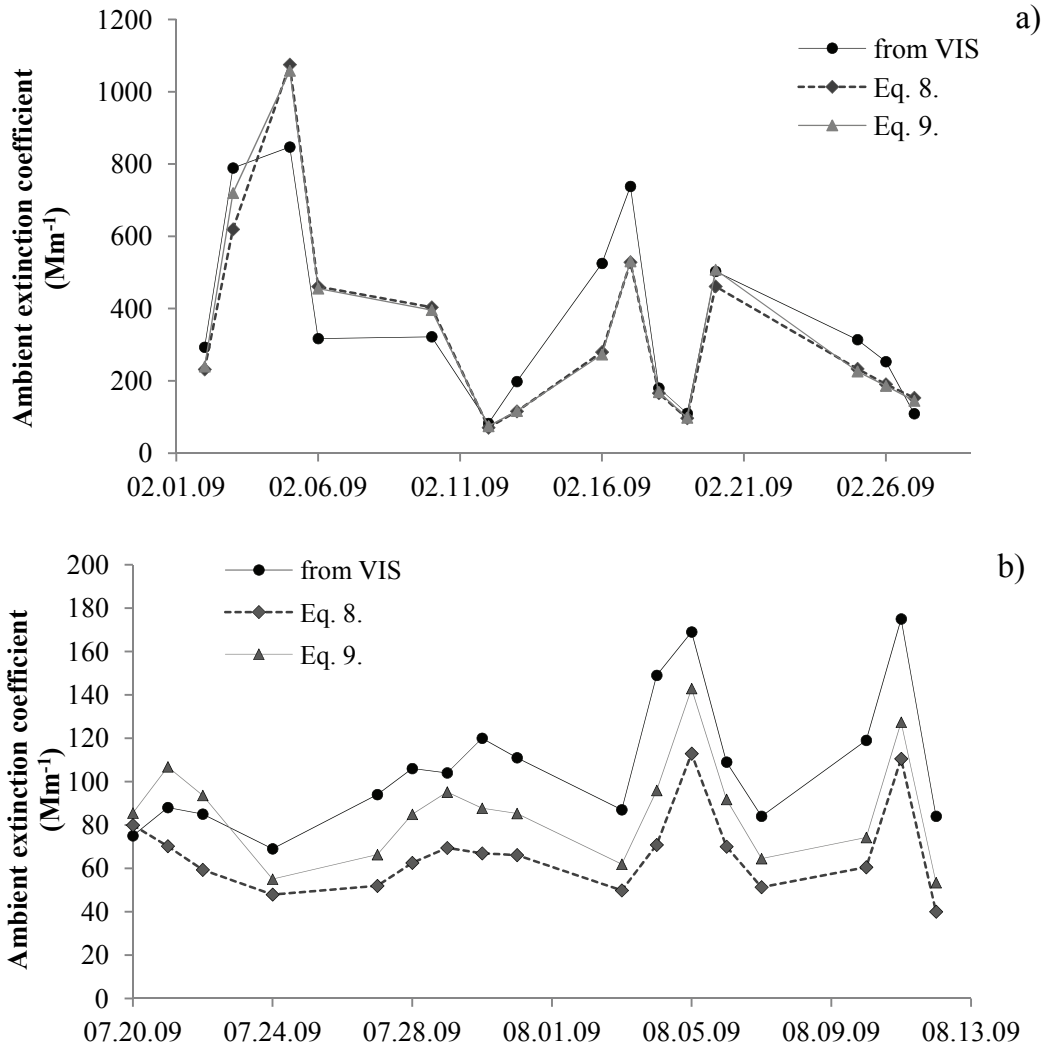

Fig. 7. Temporal variation in the ambient extinction coefficients.

Finally, we compared the three model results obtained for ambient air. We found that the results substantially differ if IMPROVE or our models are applied (see *Table 3*). The main reason for the discrepancy between modeled dry and ambient extinction coefficients can arise from the different consideration of aerosol hygroscopicity. In the case of IMPROVE, model hygroscopic growth is supposed only for ammonium sulfate and sodium nitrate content, while in our models the hygroscopicity of organic species is also involved. It supported by the well-known fact that an important part of organic compounds is hydrophilic, even water soluble. As a result, our models provide more realistic estimation of the ambient extinction coefficient compared to the IMPROVE model. This draws the attention to the significance of aerosol hygrosopicity, concerning both the inorganic and organic contents of the particles. The application of proper hygroscopic growth rate (which is a function of the chemical composition; and has significant seasonality) plays very important role in the reconstruction of ambient extinction coefficient.

4. Conclusions

Based on our results, we can conclude that visibility (extinction) data provide an efficient and inexpensive tool for the survey of long-term variations in air quality and may be utilized as a proxy for PM_{10} concentration. We have found that visibility data can generally be used to estimate atmospheric aerosol extinction coefficients, even in a retrospective manner. The closure experiment has shown that PM_{10} can be successfully estimated by chemical composition and that the PM_{10} concentration can be estimated from visibility/extinction coefficient data (using the Koschmieder theory). Our results indicate that the PM_{10} concentration (measured or modeled from the chemical composition) provides a good basis for the reconstruction of aerosol extinction coefficients. It is also shown that the derived (from VIS) and reconstructed (from PM_{10} or the aerosol chemical composition) aerosol extinction coefficients are in good accordance with each other, mainly in the case of dry aerosols. Ambient values can be estimated if the adequate hygroscopic growth rate for the aerosol extinction is considered. We have also found that a rather precise estimation of extinction coefficient can be reached if a modified version of the widely used IMPROVE formula is applied.

Acknowledgements: Authors are grateful for the support of Hungarian Scientific Research Fund (OTKA), project number K 113059.

References

Bäumer, D., Vogel, B., Versick, S., Rinke, R., Möhler, O., and *Schnaiter, M.,* 2008: Relationship of visibility, aerosol optical thickness and aerosol size distribution in an ageing air mass over South-West Germany. *Atmos. Environ. 42*, 989–998.

Cabada, J.C., Khlystov, A., Wittig, A.E., Pilinis, C. and *Pandis, S.N.,* 2004: Light scattering by fine particles during the Pittsburgh Air Quality Study: Measurements and modeling. *J. Geophys. Res. 109*, D16S03.

Cao, J.-J. Wang, Q.-Y, Chow, J.C., Watson, J.G., Tie, X.-X., Shen, Z.-X., Wang, P., and *An, Z.-S.,* 2012: Impacts of aerosol compositions on visibility impairment in Xi'an, China. *Atmos. Environ. 59,* 559–566.

Cheng, S.-H., Yang, L.-X., Zhou, X.-H., Xue, L.-K., Gao, X.-M., Zhou, Y. and Wang, W.-X., 2011: Size-fractionated water-soluble ions, situ pH and water content in aerosol on hazy days and the influences on visibility impairment in Jinan, China. *Atmos. Environ. 45,* 4631–4640

Chueinta, W. and *Hopke, P. K.*, 2001: Beta gauge for aerosol mass measurement. *Aerosol Sci. Technol. 35*, 840–843.

DeBell, L.J., Gebhart, K.A., Hand, J.L., Malm, W.C., Pitchford, M.L., Schichtel, B.A, and *White, W.H.,* 2006: IMPROVE (Interagency Monitoring of Protected Visual Environments): Spatial and Seasonal Patterns and Temporal Variability of Haze and its Constituents in the United States. Report IV CIRA Report ISSN: 0737-5352-74, Colorado State Univ., Fort Collins.

Fry, J.L., Draper, D.C., Barsanti, K.C., Smith, J.N., Ortega, J., Winkler, P.M., Lawler, M.J., Brown, S.S., Edwards, P.M., Cohen, R.C., and *Lee, L.,* 2014: Secondary organic aerosol formation and organic nitrate yield from NO_3 oxidation of biogenic hydrocarbons. *Environ. Sci. Technol. 48*, 11944−11953.

Gomišček, B., Hauck, H., Stopper, S., and *Preining, O.,* 2004: Spatial and temporal variations of PM1, PM2.5, PM10 and particle number concentration during the AUPHEP—project. *Atmos. Environ. 38*, 3917–3934

Hand, J. L., Malm, W. C., 2007: Review of aerosol mass scattering efficiencies from groundbased measurements since 1990, *J. Geophys. Res.-Atmospheres, 112,* (D18).

Hand, J.L., Copeland, S.A., Day, D.E., Dillner, A. M., Indresand, H., Malm, W.C., McDade, C.E., Moore, C.T.Jr., Pitchford, M., L., Schichtel, B.A., and *Watson, J.G.,* 2011: Spatial and Seasonal Patterns and Temporal Variability of Haze and its Constituents in the United States. Report V: June 2011. IMPROVE report, Cooperative Institute for Research in the Atmosphere, Colorado State University, Fort Collins, USA.

Hidy, G.M., Mueller, P.K., and *Tong, E.Y.,* 1978: Spatial and temporal distributions of airbone sulfate in parts of the United States, *Atmos. Environ. 12*, 735.

Horvath, H., 1992: Effect on visibility, weather and climate. In (Eds. *Radojevicc M.* and *Harrison R.M.*) Atmospheric Acidity: Sources, Consequences and abatement Elsevier Applied Science, London, 435-466.

Horvath, H., 1995: Estimation of the average visibility in central Europe, *Atmos. Environ., 29*, 241–246.

Jung, J., Lee, H., Kim, Y.J., Liu, X., Zhang, Y., Hu, M. and *Sugimoto, N.,* 2009: Optical Properties of Atmospheric Aerosols Obtained by in Situ and Remote Measurements during 2006 Campaign of Air Quality Research in Beijing (CAREBeijing-2006). *J. Geophys. Res. 114*.

Karanasiou, A., Diapouli, E., Cavalli, F., Eleftheriadis, K., Viana, M., Alastuey, A., Querol, X., Reche, C., 2011: On the quantification of atmospheric carbonate carbon by thermal/optical analysis protocols. *Atmos. Meas. Tech., 4,* 2409–2419.

Kim, K.W., 2015: Optical Properties of Size-Resolved Aerosol Chemistry and Visibility Variation Observed in the Urban Site of Seoul, Korea. *Aerosol Air Qual. Res. 15*, 271–283.

Koschmieder, H., 1924: Theorie der horizontalen sichtweite, Beitr. *Phys. frei. Atmos., 12,* 171–181.

Maenhaut, W., Raes, N., Chi, X., Cafmeyer, J., Wang, W., and *Salma, I., 2005:* Chemical composition and mass closure for fine and coarse aerosols at a kerbside in Budapest, Hungary, in spring 2002, *X Ray Spectrom., 34,* 290–296.

*Malm, W.C., Sisler, J. F., Huffman, D., Eldred, R. A.,*and *Cahill, T. A.,* 1994: Spatial and seasonal trends in particle concentration and optical extinction in the United States*, J Geophys Res. 99,* 1347–1370.

Malm, W.C., Schichtel, B.A., Barna, M.G., Gebhart, K.A., Rodriguez, M.A., Collett Jr., J.L., Carrico, C.M., Benedict, K.B., Prenni, A.J., and *Kreidenweis, S.M.,* 2013: Aerosol species concentrations and source apportionment of ammonia at Rocky Mountain National Park, *J. Air Waste Mgmt. Assn. 63,* 1245-1263.

Matta, E., Facchini, M.C., Decesari, S., Mircea, M., Cavalli, F., Fuzzi, S., Putaud, J.-P. and *Dell'Acqua, A.,* 2003: Mass closure on the chemical species in size-segregated atmospheric aerosol collected in an urban area of the Po Valley, Italy. *Atmos. Chem. Phys., 3,* 623–637.

Mészáros, E., 1999: Fundamentals of Atmospheric Aerosol Chemistry. Akadémiai Kiadó, Budapest.

Nemuc, A., Vasilescu, J., Talianu, C., Belegante, L., and *Nicolae, D.,* 2013: Assessment of aerosol's mass concentrations from measured linear particle depolarization ratio (vertically resolved) and simulations. *Atmos. Meas. Tech., 6,* 3243–3255.

Ouimette, J.R., and *Flagan R.C.,* 1982: The extinction coefficient of multicomponent aerosols. *Atmos. Environ. 16,* 2405–2419.

Pan, X.L., Yan, P., Tang, J., Ma, J.Z., Wang, Z.F., Gbaguidi, A., and *Sun, Y.L.,* 2009: Observational study of influence of aerosol hygroscopic growth on scattering coefficient over rural area near Beijing mega-city. *Atmos. Chem. Phys. 9,* 7519–7530.

Reche, C., Querol, X., Alastuey, A., Viana, M., Pey, J., Moreno, T., Rodríguez, S., Gonzalez, Y., Fernández-Camacho, R., de la Rosa, J., Dall'Osto, M., Prevôt, A.S.H., Hueglin, C., Harrison, R.M., and *Quincey, P.,* 2011: New considerations for PM, Black Carbon and particle number concentration for air quality monitoring across different European cities, *Atmos. Chem. Phys., 11,* 6207– 6227.

Seinfeld, J.H. and *Pandis, S.N.,* 1998: Atmospheric Chemistry and Physics. John Wiley & Sons.

Sillanpää, M., Frey, A., Hillamo, R., Pennanen, A.S. and *Salonen, R.O.,* 2005: Organic, elemental and inorganic carbon in particulate matter of six urban environments in Europe. *Atmos. Chem. Phys., 5*, 2869–2879.

Singh, A. and Dey, S., 2012: Influence of aerosol composition on visibility in megacity Delhi. *Atmos. Environ. 62,* 367–373.

Stelson, A.W. and *Seinfeld, J.H.,* 1981: Chemical mass accounting of urban aerosol. *Environ. Sci. Technol. 15,* 671–679.

Tao, J., Cao, J.-J., Zhang, R.-J, Zhu, L. H., Zhang T., Shi S., and *Chan, C.-Y.,* 2012: Reconstructed light extinction coefficients using chemical compositions of PM2.5 in winter in urban Guangzhou, China. *Adv. Atmos. Sci*., *29,* 359–368.

Zhou, J., Swietlicki, E. and Berg, O.H., 2001: Hygroscopic properties of aerosol particles over the central Arctic Ocean during summer. J Geophys Res. 32, 32111-32123.

Virkkula, A., Backman, J., Aalto, P.P., Hulkkonen, M., Riuttanen, L., Nieminen, T., dal Maso, M., Sogacheva, L., de Leeuw, G., and Kulmala, M., 2011: Seasonal Cycle, Size Dependencies, and Source Analyses of Aerosol Optical Properties at the SMEAR II Measurement Station in Hyytiälä, Finland. *Atmos. Chem. Phys. 11,* 4445–4468.

Waked, A., Favez, O., Alleman, L. Y., Piot, C., Petit, J.-E., Delaunay, T., Verlinden, E., Golly, B., Besombes, J.-L., Jaffrezo, J.-L., and *Leoz-Garziandia, E.,* 2014: Source apportionment of PM_{10} in a north-western Europe regional urban background site (Lens, France) using positive matrix factorization and including primary biogenic emissions, *Atmos. Chem. Phys., 14,* 3325-3346.

Wang, G., Xie, M., Hu, S., Gao, S., Tachibana, E., and *Kawamura, K.,* 2010: Dicarboxylic acids, metals and isotopic compositions of C and N in atmospheric aerosols from inland China: implications for dust and coal burning emission and secondary aerosol formation, *Atmos. Chem. Phys.,* 10, 6087–6096.